Sensors and Actuators B 150 (2010) 296–300

Contents lists available at ScienceDirect

Sensors and Actuators B: Chemical

journal homepage: www.elsevier.com/locate/snb

Wafer-scale synthesis of graphene by chemical vapor deposition and its application in hydrogen sensing

Wei Wu[a,b], Zhihong Liu[b], Luis A. Jauregui[c,d], Qingkai Yu[a,b,*], Rajeev Pillai[a], Helin Cao[c,e], Jiming Bao[b], Yong P. Chen[c,d,e], Shin-Shem Pei[a,b]

[a] Center for Advanced Materials, University of Houston, Houston, TX 77204, USA
[b] Department of Electrical and Computer Engineering, University of Houston, Houston, TX 77204, USA
[c] Birck Nanotechnology Center, Purdue University, West Lafayette, IN 47907, USA
[d] School of Electrical and Computer Engineering, Purdue University, West Lafayette, IN 47907, USA
[e] Department of Physics, Purdue University, West Lafayette, IN 47907, USA

ARTICLE INFO

Article history:
Received 7 March 2010
Received in revised form 8 June 2010
Accepted 30 June 2010
Available online 16 July 2010

Keywords:
Graphene
Chemical vapor deposition
Gas sensor

ABSTRACT

Graphene with a large area was synthesized on Cu foils by chemical vapor deposition under ambient pressure. A 4″ × 4″ graphene film was transferred onto a 6″ Si wafer with a thermally grown oxide film. Raman mapping indicates monolayer graphene dominates the transferred graphene film. Gas sensors were fabricated on a 4 mm × 3 mm size graphene film with a 1 nm palladium film deposited for hydrogen detection. Hydrogen in air with concentrations in 0.0025–1% (25–10,000 ppm) was used to test graphene-based gas sensors. The gas sensors based on palladium-decorated graphene films show high sensitivity, fast response and recovery, and can be used with multiple cycles. The mechanism of hydrogen detection is also discussed.

1. Introduction

Graphene [1,2], a single atomic layer of graphite, is the building block of all sp^2 bonded carbon materials including graphite as well as carbon nanotubes. The explosion of recent interests in graphene is in a large part due to its exceptional electronic properties [3–8] demonstrated experimentally and its potential application, such as nanoelectronic devices [9] and chemical/bio-sensors [10,11]. While the first electrically isolated graphene was fabricated by mechanical exfoliation of graphite [7], a large amount of recent effort has been devoted to develop methods to synthesize graphene at large scale for practical electronic applications. A variety of methods, such as epitaxial growth on SiC [12,13], chemical vapor deposition (CVD) on metals [14–21], and numerous solution-based chemical approaches [22–25] have been explored. One of the most important and challenging goals is to grow graphene at large scale with uniform thickness [13,18].

Carbon materials are useful as chemical/bio-sensors since the environmental sensitivity of carbon-based molecules can be efficiently tailored by synthetic chemistry techniques [26]. Chemical/bio-sensors based on carbon nanotubes (CNTs) have already been extensively studied in a decade [27–30]. However, the diversity in CNTs' structure and chirality may lead to varied device characteristics, and thereby cause device reliability issues [31]. On the contrary, graphene has a great potential to resolve these problems. Graphene is a strictly two-dimensional (2D) material and, as such, enables devices based on graphene to have an identical performance on a large scale. The fabrication of chemical/bio-sensors in field effect transistor type structures based on graphene in large scale is also simpler than that of SWNT. In addition, with the 2D structure, the monolayer graphene has its whole volume exposed to the environment, which can maximize the sensing effect. The principle of graphene devices is based on changes in device conductance due to chemical or biological species adsorbed on the surface of graphene, acting as electron donors or acceptors. Recently, graphene-based gas molecule sensors and biosensors have been reported [10,11,32].

In this paper, we report wafer-scale synthesis of monolayer graphene by CVD under ambient pressure and explore its application in gas sensors. With the progress of synthesis of wafer-scale graphene with uniform thickness, sensors based on the graphene are expected to have an identical performance. Therefore, the commercialization of graphene-base chemical/bio-sensors could be realizable.

* Corresponding author at: Center for Advanced Materials, University of Houston, 724 Science & Research BLDG 1, Houston, TX 77204, USA.
Tel.: +1 713 7433621; fax: +1 713 7477724.
E-mail address: qyu2@uh.edu (Q. Yu).

0925-4005/$ – see front matter © 2010 Elsevier B.V. All rights reserved.
doi:10.1016/j.snb.2010.06.070

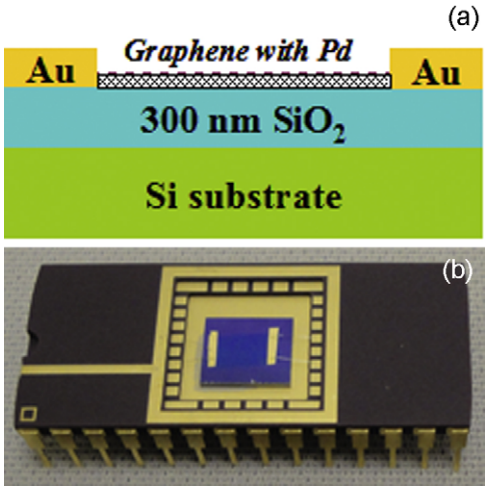

Fig. 1. (a) Schematic cross-sectional view of graphene deposited with Pd nanoparticles on SiO_2/Si substrate for H_2 sensor. (b) Photograph of a typical H_2 sensor device. The size of SiO_2/Si substrate is about 1 cm.

2. Experimental

2.1. Graphene growth and Raman characterization

Graphene was synthesized on Cu foils and transferred to Si/SiO_2 wafers using procedures analogous to those in published literature [18] and in our previous work [14,15,21]. Briefly, the procedure is described as follows. Graphene was grown by thermal CVD on a Cu foil, at a temperature of 1000 °C and under 1 atm pressure with methane as the precursor gas. A quartz tube with 2″ diameter was used as the reaction chamber for our CVD system. Cu foils were rolled up in a roll, but without the rolled-up layers touching to each other. Following the growth, PMMA was spun on graphene/Cu substrate to form PMMA/graphene/Cu sandwich structure. Later, Cu foil was etched away using an iron nitrate aqua solution. After the Cu foil was completely etched away, graphene with PMMA/graphene film was transferred onto a Si wafer with 300 nm thermally grown SiO_2. The PMMA was then removed by repeatedly rinsing the film in acetone.

Our Raman measurements were performed with a Horiba LabRam confocal Raman microscope with a motorized sample stage for Raman mapping. The wavelength of the excitation laser used was 532 nm and the power kept low enough (typically on the order of 1 mW at the sample surface) in the "linear" regime, that is, further reducing the power would not give appreciable change in the intensity ratios (defined below) between relevant Raman bands (but will give more noise in the spectra). The laser spot size is ~0.6 μm for the 100× objective used.

2.2. Gas sensor device fabrication and testing

The schematic view of a hydrogen sensor based on Pd modified graphene is shown in Fig. 1a. CVD grown graphene with a typical size of 3 mm × 4 mm was transferred onto a highly doped Si wafer covered by a 300 nm-thick SiO_2 film. The graphene sample on SiO_2/Si was then decorated with a thin Pd film (1 nm thickness) using electron beam evaporation. To define the contacts, Ti/Au (5 nm/100 nm) films were also deposited by electron beam evaporation through a shadow mask. Subsequently, the sensor sample was assembled into a chip carrier by wire bonding, as shown in Fig. 1b.

The sensor devices were characterized in a home-made testing chamber flowing a mixture of hydrogen and air with a flow rate of 5000 sccm at atmospheric pressure and room temperature. The concentration of hydrogen was varied by controlling the flow rates of the two gases using MKS mass flow controllers. The variation of sensor resistance was measured using a computer-controlled Keithley 2400 source meter. The carrier type and carrier density in our graphene sensor were characterized in hydrogen environment at different concentrations by Hall effect measurements. For Hall effect measurements, a square graphene sample (1 cm × 1 cm) with Ti/Au contacts at four corners was placed in a glass tube with gas inlet and outlet. The glass tube was entirely covered by black tapes to eliminate the influence of light in the environment.

3. Results and discussions

3.1. Raman characterization

Raman spectroscopy is a powerful, yet relatively simple method to characterize the thickness and crystalline quality of graphene layers [17–19]. We have performed Raman spectroscopy and Raman mapping on the CVD graphene films transferred to SiO_2/Si. In particular, we have used spatially resolved Raman measurements to probe the uniformity of our large-scale CVD graphene. Fig. 2a–c shows a representative Raman map showing the intensity of D, G and 2D bands measured in a 10 μm × 10 μm area of a CVD graphene sample (the corresponding optical microscope image of the scanned area is shown as the inset of Fig. 2a). To extract the intensity of a given band, I_x (where x = D, G, or 2D), we performed a best Lorentzian ($f(x) = y_0 + Aw/(w^2 + 4(x - x_0)^2)$) fit to the peak over the corresponding range. The intensity (I_x) is defined by the amplitude value (A/w) of the Lorentzian function fit. We used intervals 1320–1380, 1560–1620 and 2640–2720 cm^{-1} as the range of the D, G, and 2D bands for the Lorentzian function fit, respectively. By comparing Fig. 3a–c, we can learn that the intensity maps of G and 2D bands are correlated, while the intensity map of D band (signal from defects) is not correlated to those of G and 2D bands (both signals from graphene lattice). In the sample, the locations where G band has a high density are also the locations where 2D band has a high density. The possible reason is the spatially non-uniform adhesion. The images by He ion microscope (not shown here), indicates the transferred graphene does not spatially uniformly adhere to the substrate. The adhesion between graphene and a substrate can affect the intensity of Raman spectra. However, D band is always low owing to the high quality of the graphene and it intends to show a noisy feature. Fig. 2d shows the Raman map of I_D/I_G of the same area scanned in Fig. 2a. The mean value of I_D/I_G is less than 0.1, which indicate low defect density in the graphene film. It is known that I_{2D}/I_G is a sensitive probe of the number of graphene layers [17–19]. For example, our measurements (under similar experimental conditions as we used in Fig. 2) on exfoliated graphene layers gave typical I_{2D}/I_G ~2–3 for monolayer samples and I_{2D}/I_G slightly lower than 1 for bilayers. Previous studies [18] of CVD-grown graphene (transferred from Cu) have taken a I_{2D}/I_G ~2 to indicate monolayer graphene, $2 > I_{2D}/I_G > 1$ for bilayer and $I_{2D}/I_G < 1$ for multilayers (it has also been noted that due to possible stacking disorder, it can be more difficult to determine the exact number of CVD-grown graphene layers from the Raman spectrum compared with exfoliated graphene [19]). We find that ~99% of the area mapped show $I_{2D}/I_G > 2$, ~93% of the area mapped show $I_{2D}/I_G > 3$ and about half of the area show $I_{2D}/I_G > 4$ (the medium value). Based on our I_{2D}/I_G data, we conclude that most of the area mapped is monolayer graphene. We also notice that, even in locations with $I_{2D}/I_G > 2$, believed to indicate monolayer, we can still observe substantial variation in I_{2D}/I_G (as seen, for example, in several Raman spectra in Fig. 2f measured from the corresponding marked spots in Fig. 2e). We speculate that one possible reason for this variation and sometimes very large I_{2D}/I_G (e.g.

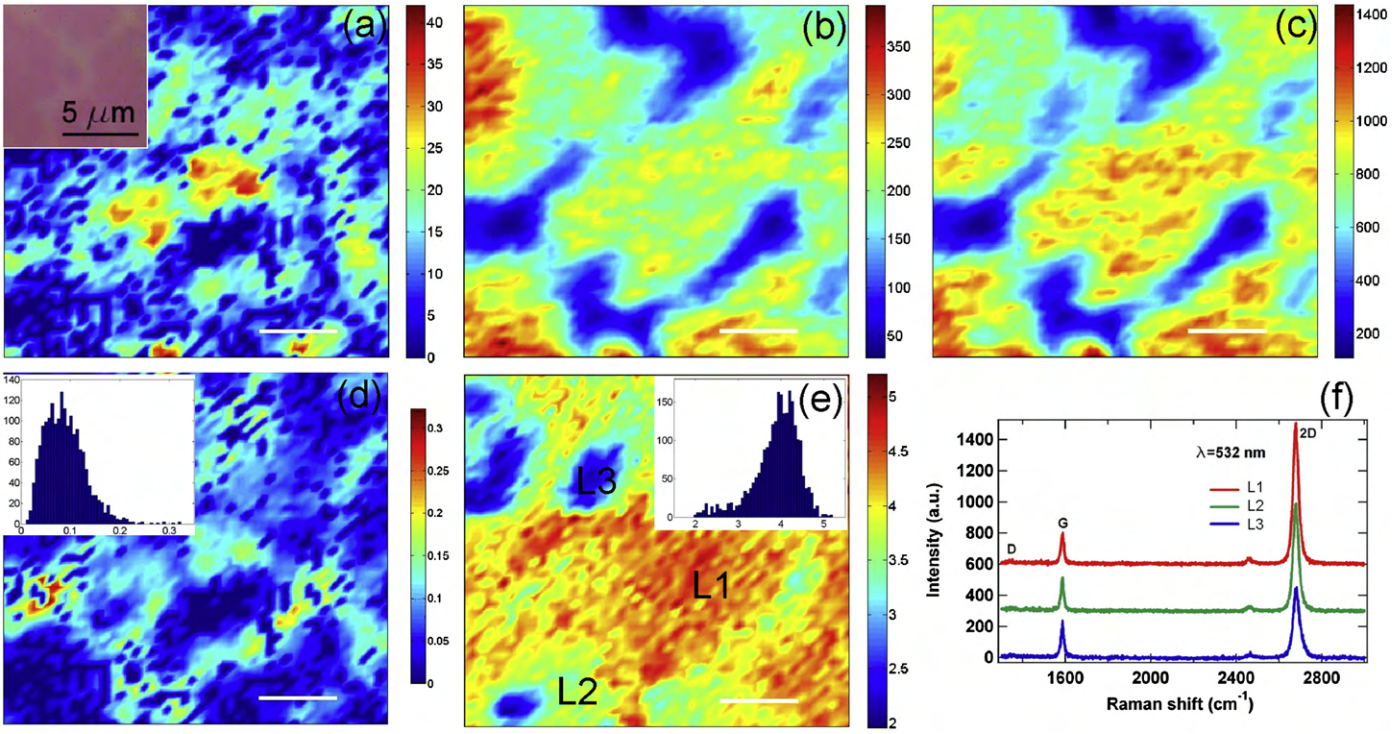

Fig. 2. Raman characterization of CVD graphene transferred to a Si/SiO_2 substrate. All of the Raman maps for I_D (a), I_G (b), I_{2D} (c), I_D/I_G (d), and I_{2D}/I_G, were measured at same location in a 10 μm × 10 μm area. The inset in (a) shows the optical image of the area mapped. The insets in (d) and (e) show histogram of I_D/I_G and I_{2D}/I_G, respectively. In the histograms, *x*-axis indicates the ratios of I_D/I_G and I_{2D}/I_G and *y*-axis indicates counts. All of scale bars in maps are 2 μm, except (a) inset. Raman spectra shown in (f) measured from the marked location L1, L2 and L3 in (e), respectively. The D, G, and 2D bands are labeled in the spectra.

>5) may also be the spatially non-uniform adhesion between the transferred graphene film and the underlying substrate (SiO_2), as the graphene-substrate interaction could strongly affect I_{2D}/I_G [33]. The adhesion can significantly affect G and 1D band, but with different extents. The disorder-induced D band in the spectra shown in Fig. 2f is seen to be very small, indicating high crystalline quality of the graphene. We have also obtained qualitatively similar Raman maps from many areas randomly selected from different locations of a large-scale CVD graphene film. Several of these areas have been subsequently fabricated into devices and an independent and more unambiguous verification of monolayer graphene has been performed using quantum Hall measurements [14]. Our results suggest that our CVD graphene films have excellent quality and uniformity, consisting mainly of monolayer.

3.2. Hydrogen sensor properties and sensor mechanism

The hydrogen sensing capability is experimentally tested by recording sensor resistance change when the sensor is exposed to hydrogen gas with different concentrations. The sensor sensitivity is defined by sensitivity = $(R_{peak} - R_0)/R_0 \times 100\%$, where R_{peak} is the highest sensor resistance in hydrogen gas and R_0 is the

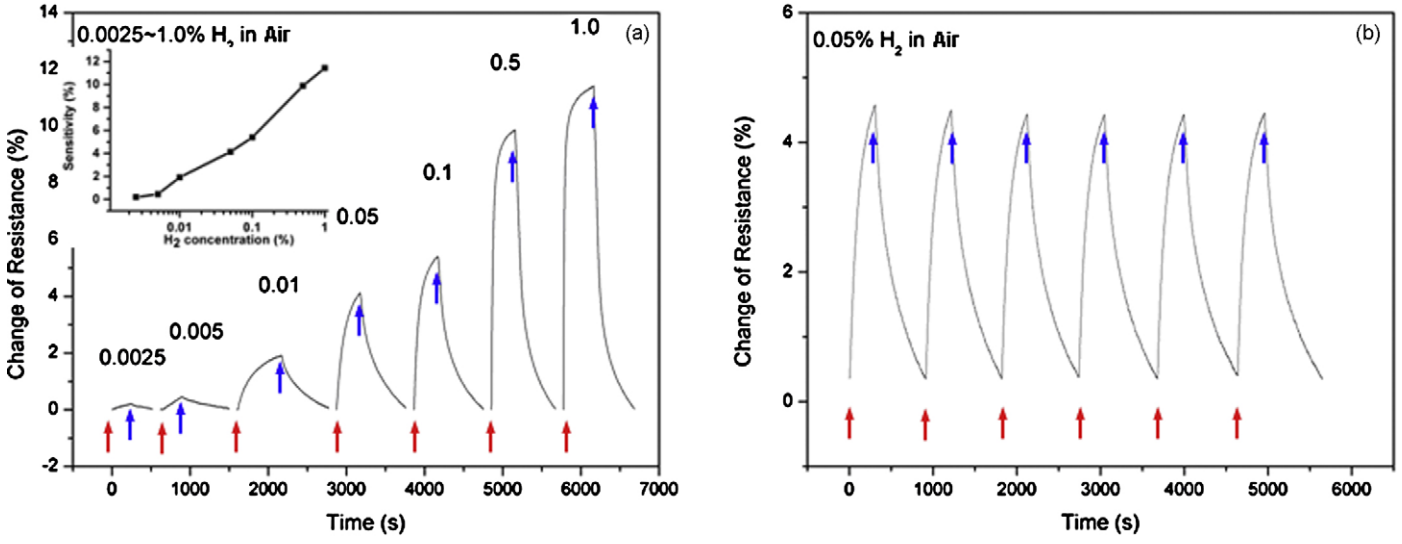

Fig. 3. (a) The change of source-drain current of sensor to H_2 with difference concentration. The inset shows the sensitivities of the sensor for hydrogen at different concentrations. (b) The change of source-drain current of sensor to 0.05% (500 ppm) H_2 in 6 times of gas on/off cycles. Red arrows indicate the time of hydrogen on and blue arrows indicate the time of gas off. (For interpretation of the references to colour in this figure legend, the reader is referred to the web version of the article.)

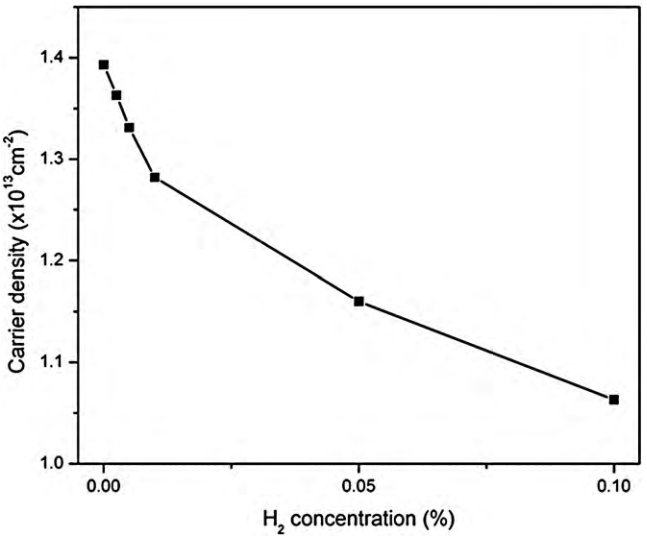

Fig. 4. Carrier density in graphene sensor vs. H_2 concentration.

resistance in air. Fig. 3a shows the percentage of the sensor resistance change to various hydrogen concentrations from 0.0025% to 1% (25–10,000 ppm). The concentrations in details are labeled above each peak in Fig. 3a. Before turning on hydrogen, only air flowed through the testing chamber. After turning on hydrogen, the resistance of the graphene sensor increased with time upon the exposure to hydrogen. After 300 s, hydrogen was shut off and only air flowed through the testing chamber for several hundred seconds to let the resistance recover the original level. The graphene sensor was tested in hydrogen with varied concentrations in the order from low to high concentrations. We also tested the graphene sensors without Pd deposition and could not observe non-trivial change of the sensor's resistivity. The sensitivity of the sensor to hydrogen concentration is roughly linear in a logarithm coordinate, as shown in the inset of Fig. 3a. The hydrogen sensor shows more than 10% increase of resistance to the exposure to 1% hydrogen concentration. For much lower concentration of hydrogen (minimum 0.0025% (25 ppm) hydrogen in the case investigated), there is also an observable signal with a corresponding resistance increase of 0.2%. As the hydrogen concentration decreases, the number of adsorbed hydrogen molecules is reduced, and therefore, the corresponding sensitivity also decreases. The response and recovery times are defined as the time durations to reach 90% of the range of resistance change since the beginning of H_2 gas flow and end of H_2 gas flow, respectively. Whenever the sensor is exposed to hydrogen, a quick increase of resistance is observed. For example, for the sensor response to 0.05% (500 ppm) hydrogen, the response time is 213 s and the resistance of the sensor increased 1% in less than 30 s. After tuning hydrogen off, the resistance decrease fast and the measured recovery time is 463 s. Fig. 4b shows the sensor response to 0.05% (500 ppm) hydrogen concentration for six cycles. The sensitivity measured is around 4.10% for each cycle. The resistance of the sensor recovers to its original value within 10 min when hydrogen gas is completely closed and the test chamber is purged with air. We also used argon to purge the sample after turning off hydrogen and found that the sensor's resistance recovered much slower.

The sensing mechanism of gas sensors based on graphene can be attributed to the change of carrier density in graphene induced by palladium hydride (PdH_x). With Pd deposition on graphene by electron beam evaporation, discrete Pd nanoparticles form on graphene. When the Pd-decorated graphene is exposed to hydrogen, Pd atoms can be converted to PdH_x. PdH_x on graphene has an electrical dipole structure [34], i.e. the charge is positive at hydrogen side and electrons accumulates at the interface between Pd and carbon. According to Hall effect measurements, our CVD graphene samples were found to be p-type, which is common in as-fabricated graphene devices [7]. The electrons accumulating at the interface of Pd and graphene can neutralize holes in graphene, therefore, reduce the p-type carrier density. Fig. 4 shows that the p-type carrier density decreases with concentration of hydrogen in air in the range of 0–0.1%. Lower carrier density is the reason that resistance increases with hydrogen concentration. The formation of dipole structure by PdH_x plays a critical role in hydrogen sensing for our graphene sensors. According to our testing results of graphene sensor without Pd deposition, hydrogen only has very limited interaction directly with graphene. Increased resistivity with hydrogen concentration has also been observed in CNTs-based hydrogen sensors [34–36]. The resistance of our sensor exposed to hydrogen recovered much slower in pure argon than in air. It is expected that oxygen in air greatly enhances the decomposition of PdH_x, which can be described as $1/4O_2 + Pd_{active}/H \rightarrow Pd_{active} + 1/2H_2O$ [34]. It should also be noticed that Pd is a catalyst to decompose H_2. However, it is hard to form chemisorption between graphene and hydrogen radical at room temperature [35]. Therefore, it is hard for the graphene/H_2 to interact to induce the change of sensor conductance.

4. Conclusion

We synthesized graphene with a large area on a Cu foil at a temperature of 1000 °C under 1 atm pressure with methane as the precursor gas by thermal CVD. Although only $4'' \times 4''$ graphene film was demonstrated, the size of graphene film, which can be synthesized by this approach, is not limited by the size of CVD chamber at all owing to the rolled-up Cu foil during synthesis. Raman spectrum shows 99% area of the film has ratio of 2D band to G band larger than 2, which indicates most of film is a monolayer. Thanks to the synthesis of wafer-scale graphene with uniform thickness, sensors based on the graphene are expected to have an identical performance comparing with other nanomaterials, such as CNTs. Hydrogen sensors were demonstrated on Pd-decorated CVD graphene films. The hydrogen sensors show high sensitivity, fast response and recovery, and are usable for multiple cycles. The mechanism of hydrogen detection can be attributed to carrier density in graphene induced by PdH_x.

Acknowledgements

Acknowledgment is made to National Science Foundation 0907336, Miller Family Endowment, Midwest Institute for Nanoelectronics Discovery (MIND), Indiana Economic Development Corporation (IEDC), and American Chemical Society Petroleum Research Fund (PRF).

References

[1] A.K. Geim, Graphene: status and prospects, Science 324 (2009) 1530–1534.
[2] A.K. Geim, K.S. Novoselov, The rise of graphene, Nature Materials 6 (2007) 183–191.
[3] A.H. Castro Neto, F. Guinea, N.M.R. Peres, K.S. Novoselov, A.K. Geim, The electronic properties of graphene, Reviews of Modern Physics 81 (2009) 109–162.
[4] Z.H. Chen, Y.M. Lin, M.J. Rooks, P. Avouris, Graphene nano-ribbon electronics, Physica E-Low-Dimensional Systems & Nanostructures 40 (2007) 228–232.
[5] M.Y. Han, B. Ozyilmaz, Y.B. Zhang, P. Kim, Energy band-gap engineering of graphene nanoribbons, Physical Review Letters 98 (2007).
[6] K.S. Novoselov, A.K. Geim, S.V. Morozov, D. Jiang, M.I. Katsnelson, I.V. Grigorieva, S.V. Dubonos, A.A. Firsov, Two-dimensional gas of massless Dirac fermions in graphene, Nature 438 (2005) 197–200.
[7] K.S. Novoselov, A.K. Geim, S.V. Morozov, D. Jiang, Y. Zhang, S.V. Dubonos, I.V. Grigorieva, A.A. Firsov, Electric field effect in atomically thin carbon films, Science 306 (2004) 666–669.

[8] Y.B. Zhang, Y.W. Tan, H.L. Stormer, P. Kim, Experimental observation of the quantum Hall effect and Berry's phase in graphene, Nature 438 (2005) 201–204.
[9] P. Avouris, Carbon nanotube electronics and photonics, Physics Today 62 (2009) 34–40.
[10] Y. Ohno, K. Maehashi, Y. Yamashiro, K. Matsumoto, Electrolyte-gated graphene field-effect transistors for detecting pH protein adsorption, Nano Letters 9 (2009) 3318–3322.
[11] F. Schedin, A.K. Geim, S.V. Morozov, E.W. Hill, P. Blake, M.I. Katsnelson, K.S. Novoselov, Detection of individual gas molecules adsorbed on graphene, Nature Materials 6 (2007) 652–655.
[12] C. Berger, Z.M. Song, X.B. Li, X.S. Wu, N. Brown, C. Naud, D. Mayou, T.B. Li, J. Hass, A.N. Marchenkov, E.H. Conrad, P.N. First, W.A. de Heer, Electronic confinement and coherence in patterned epitaxial graphene, Science 312 (2006) 1191–1196.
[13] K.V. Emtsev, A. Bostwick, K. Horn, J. Jobst, G.L. Kellogg, L. Ley, J.L. McChesney, T. Ohta, S.A. Reshanov, J. Rohrl, E. Rotenberg, A.K. Schmid, D. Waldmann, H.B. Weber, T. Seyller, Towards wafer-size graphene layers by atmospheric pressure graphitization of silicon carbide, Nature Materials 8 (2009) 203–207.
[14] H. Cao, Q. Yu, L.A. Jauregui, J. Tian, W. Wu, Z. Liu, R. Jalilian, D.K. Benjamin, Z. Jiang, J. Bao3, S.-S. Pei, Y.P. Chen, Electronic transport in chemical vapor deposited graphene synthesized on Cu: quantum Hall effect and weak localization, Applied Physics Letters 96 (2010) 122106.
[15] Q. Yu, J. Lian, S. Siriponglert, H. Li, Y.P. Chen, S.-S. Pei, Graphene segregated on Ni surfaces and transferred to insulators, Applied Physics Letters 93 (2008) 113103.
[16] L.G. De Arco, Y. Zhang, A. Kumar, C.W. Zhou, Synthesis, transfer, and devices of single- and few-layer graphene by chemical vapor deposition, IEEE Transactions on Nanotechnology 8 (2009) 135–138.
[17] K.S Kim, Y. Zhao, H. Jang, S.Y. Lee, J.M. Kim, J.H. Ahn, P. Kim, J.Y. Choi, B.H. Hong, Large-scale pattern growth of graphene films for stretchable transparent electrodes, Nature 457 (2009) 706–710.
[18] X.S. Li, W.W. Cai, J.H. An, S. Kim, J. Nah, D.X. Yang, R. Piner, A. Velamakanni, I. Jung, E. Tutuc, S.K. Banerjee, L. Colombo, R.S. Ruoff, Large-area synthesis of high-quality and uniform graphene films on copper foils, Science 324 (2009) 1312–1314.
[19] A. Reina, X.T. Jia, J. Ho, D. Nezich, H.B. Son, V. Bulovic, M.S. Dresselhaus, J. Kong, Large area, few-layer graphene films on arbitrary substrates by chemical vapor deposition, Nano Letters 9 (2009) 30–35.
[20] H. Cao, Q. Yu, R. Colby, D. Pandey, C. Park, J. Lian, D. Zemlyanov, I. Childres, V. Drachev, E.A. Stach, M. Hussain, H. Li, S.-S. Pei, Y.P. Chen, Large-scale graphitic thin films synthesized on Ni and transferred to insulators: structural and electronic properties, Journal of Applied Physics 107 (2010) 044310.
[21] Q. Yu, J. Lian, S. Siriponglert, H. Li, Y. Chen, S.-S. Pei, Graphene Synthesis by Surface Segregation on Ni and Cu, arXiv, 0804.1778v1, 2008.
[22] S. Gilje, S. Han, M. Wang, K.L. Wang, R.B. Kaner, A chemical route to graphene for device applications, Nano Letters 7 (2007) 3394–3398.
[23] C. Gomez-Navarro, R.T. Weitz, A.M. Bittner, M. Scolari, A. Mews, M. Burghard, K. Kern, Electronic transport properties of individual chemically reduced graphene oxide sheets, Nano Letters 7 (2007) 3499–3503.
[24] L.J. Cote, F. Kim, J.X. Huang, Langmuir-Blodgett assembly of graphite oxide single layers, Journal of the American Chemical Society 131 (2009) 1043–1049.
[25] S. Park, R.S. Ruoff, Chemical methods for the production of graphenes, Nature Nanotechnology 4 (2009) 217–224.
[26] K. Balasubramanian, M. Burghard, Biosensors based on carbon nanotubes, Analytical and Bioanalytical Chemistry 385 (2006) 452–468.
[27] J. Kong, N.R. Franklin, C.W. Zhou, M.G. Chapline, S. Peng, K.J. Cho, H.J. Dai, Nanotube molecular wires as chemical sensors, Science 287 (2000) 622–625.
[28] R.J. Chen, Y.G. Zhang, D.W. Wang, H.J. Dai, Noncovalent sidewall functionalization of single-walled carbon nanotubes for protein immobilization, Journal of the American Chemical Society 123 (2001) 3838–3839.
[29] J. Kong, M.G. Chapline, H.J. Dai, Functionalized carbon nanotubes for molecular hydrogen sensors, Advanced Materials 13 (2001) 1384–1386.
[30] K. Besteman, J.O. Lee, F.G.M. Wiertz, H.A. Heering, C. Dekker, Enzyme-coated carbon nanotubes as single-molecule biosensors, Nano Letters 3 (2003) 727–730.
[31] Z.H. Chen, J. Appenzeller, J. Knoch, Y.M. Lin, P. Avouris, The role of metal-nanotube contact in the performance of carbon nanotube field-effect transistors, Nano Letters 5 (2005) 1497–1502.
[32] N. Mohanty, V. Berry, Graphene-based single-bacterium resolution biodevice and DNA transistor: interfacing graphene derivatives with nanoscale and microscale biocomponents, Nano Letters 8 (2008) 4469–4476.
[33] S. Berciaud, S. Ryu, L.E. Brus, T.F. Heinz, Probing the intrinsic properties of exfoliated graphene: Raman spectroscopy of free-standing monolayers, Nano Letters 9 (2009) 346–352.
[34] Y.G. Sun, H.H. Wang, M.G. Xia, Single-walled carbon nanotubes modified with Pd nanoparticles: unique building blocks for high-performance, flexible hydrogen sensors, Journal of Physical Chemistry C 112 (2008) 1250–1259.
[35] A.Z Sadek, C. Zhang, Z. Hu, J.G. Partridge, D.G. McCulloch, W. Wlodarski, K. Kalantar-zadeh, Uniformly dispersed Pt–Ni nanoparticles on nitrogen-doped carbon nanotubes for hydrogen sensing, Journal of Physical Chemistry C 114 (2010) 238–242.
[36] M.K. Kumar, S. Ramaprabhu, Nanostructured Pt functionlized multiwalled carbon nanotube based hydrogen sensor, Journal of Physical Chemistry B 110 (2006) 11291–11298.

Biographies

Wei Wu received the BE degree in Inorganic Materials Engineering, and the MS degree in Materials Science from East China University of Science and Technology, Shanghai, China, in 2005 and 2008, respectively. He is currently working toward the PhD degree in Electrical Engineering at the University of Houston. His research interests are synthesis of nanomaterials, including graphene, tungsten and silicon nanostructures, nanofabrication and nanodevices.

Zhihong Liu received his Bachelor's degree (2003) and PhD (2008) from Zhejiang University in Department of Materials Science and Engineering. He is working as a postdoc fellow in University of Houston after 2008. His current research interests are mainly focused on growing Graphene and semiconductor nanostructures by chemical vapor deposition method, as well as characterization and application of these nanostructures.

Luis A. Jauregui obtained his BSc from National University of Engineering (Lima, Peru). As an undergraduate student he worked in Ab initio calculation of sensors for DNA sequencing and towards molecular electronics. He is currently pursuing a PhD degree in Electrical Engineering at Purdue University. As a PhD student his research interest are in the area of thermal and electronic transport of devices based on low dimensional materials (graphene, CNTs and nanowires), as well as nanoelectromechanical systems; intended for sensing, analog and/or digital device applications.

Qingkai Yu is currently a research assistant professor of Electrical Engineering and project leader in Center for Advanced Materials in the University of Houston. Dr. Yu received his PhD degree in Electrical Engineering from the University of Houston. His research interests include materials synthesis, nanofabrication and nanodevices.

Rajeev Pillai received his BE Electronics and Communication Engineering from Bharathiar University, India, and his MS and PhD in Electrical Engineering from the University of Houston, Texas, USA. He currently holds a postdoctoral fellow position with the University of Houston and a Research Scientist position with Integrated Micro Sensors. He has in depth knowledge and experience in developing thin film based solid state sensors and devices for various optical, chemical and physical applications. His current research focuses on devices based on III-Nitride thin films and graphene monolayers.

Helin Cao obtained his MSc in 2006 from University of Science and Technology of China (USTC) in the field of quantum optics. Presently he is pursuing his PhD in Yong Chen's group, Physics Department of Purdue University. His current research interests are physics properties of graphene-based nano-materials and nano-electronics.

Jiming Bao is an assistant professor in the Department of Electrical and Computer Engineering at the University of Houston. He obtained his PhD in applied physics from the University of Michigan in 2003. His research interests include nanomaterials and their device applications.

Yong P. Chen is currently the Miller Family Assistant Professor of Nanoscience and Physics and Assistant Professor Courtesy of Electrical and Computer Engineering at Purdue University. He directs the Quantum Matter and Devices Laboratory (http://www.physics.purdue.edu/quantum) and is also a faculty affiliate of Purdue's Birck Nanotechnology Center. Dr. Chen received his PhD in electrical engineering from Princeton University in 2005 and was a postdoctoral fellow in physics at Rice University from 2005 to 2007. He is a recipient of NSF CAREER Award, IBM Faculty Award, DOD DTRA Young Investigator Award and American Chemical Society PRF Young Investigator Award.

Shin-Shem Pei received a BS degree in Physics from the National Taiwan University, China in 1970 and a PhD in Solid State Physics from the State University of New York at Stony Brook in 1978. Dr. Pei joined the UH faculty in 1994 as a Professor. Prior to joining UH, Dr. Pei was the Head of the Materials and Processing Research Department at AT&T Bell Laboratories, Murray Hill, NJ. He has published and lectured on a variety of semiconductor and superconducting devices and materials. Five patents on various optoelectronics technologies have been awarded to him.